



Analysis of the mixed-field radiation environment at CHARM using FLUKA

Helena Grete Lillepalu

Supervisors: Daniel Prelicpean, Andreas Waets

Abstract

This project within the Radiation to Electronics (R2E) project quantifies the impact of the beam energy on the mixed radiation field at the CHARM facility, using the Monte Carlo code FLUKA. The nominal 24 GeV proton beam has been simulated at 21, 18, 15, 12, 9 and 1 GeV, for two configurations without shielding: copper and no target.

Keywords: CHARM, FLUKA, R2E, Monte Carlo Simulation.

Contents

1	Introduction	2
2	CHARM	2
3	Explored quantities	3
3.1	Total Ionising Dose	3
3.2	Fluence Per Unit Lethargy	3
4	Results For Copper Target Configuration	3
4.1	Total Ionising Dose	4
4.2	Fluence Per Unit Lethargy	4
5	Results For No Target Configuration	9
5.1	Total Ionising Dose	9
5.2	Fluence Per Unit Lethargy	10
6	Conclusion	17

1 Introduction

The CERN High Energy Accelerator Mixed-field (CHARM) facility [1, 2] is used for testing electronic devices in different clearly described radiation environments. It is capable of reproducing a range of real radiation fields, including the ones in accelerator complexes or even in space. To better understand and predict the field in the facility a Monte Carlo simulation software, called FLUKA [3–5], is used. This enables to calculate significant quantities for electronics testing in different configurations and test locations [6, 7]. The aim of this project was to quantify differences in the mixed radiation field at CHARM facility depending on the beam energy. In the scope of this project, two test configurations were explored: copper target with no shielding (CuOOOO) and no target with no shielding (NTOOOO).

2 CHARM

The CHARM facility is located in the Proton Synchrotron East Area hall at CERN’s Meyrin site. From the Proton Synchrotron a 24 GeV proton beam is directed to various facilities, CHARM being one of them. The main purpose of the facility is to provide a place for testing electronic devices in various well-controlled mixed-radiation fields. One of the possible ways of varying the field is the use of different target materials. In the CHARM facility there are 3 different options for a target material: aluminium, aluminium with holes and copper. Another possibility is evidently using no target. For shielding, movable shielding plates are used, which are made of either concrete or iron. In the case of maximum shielding, all 4 shielding plates (2 made of concrete and 2 of stainless steel) are in place, for half shielding only one copper and one aluminium plates are used and in the case of no shielding none of the plates are in place. The facility has a number of test locations for placing the device which is to be tested, which is another way of varying the radiation field. In Figure 1, marked with red numbers, the 13 possible rack positions are depicted, from which some are directly in the proton beam and others behind the shielding. In the locations that are closer to the beam the field is dominated by the charged hadrons, and in the locations that are perpendicular to the target are dominated by neutrons. As the field passes through the shielding, the energy of the field decreases and the composition of the beam changes. Finally, perhaps the most straightforward way of changing the radiation field is modifying the energy of the primary beam.

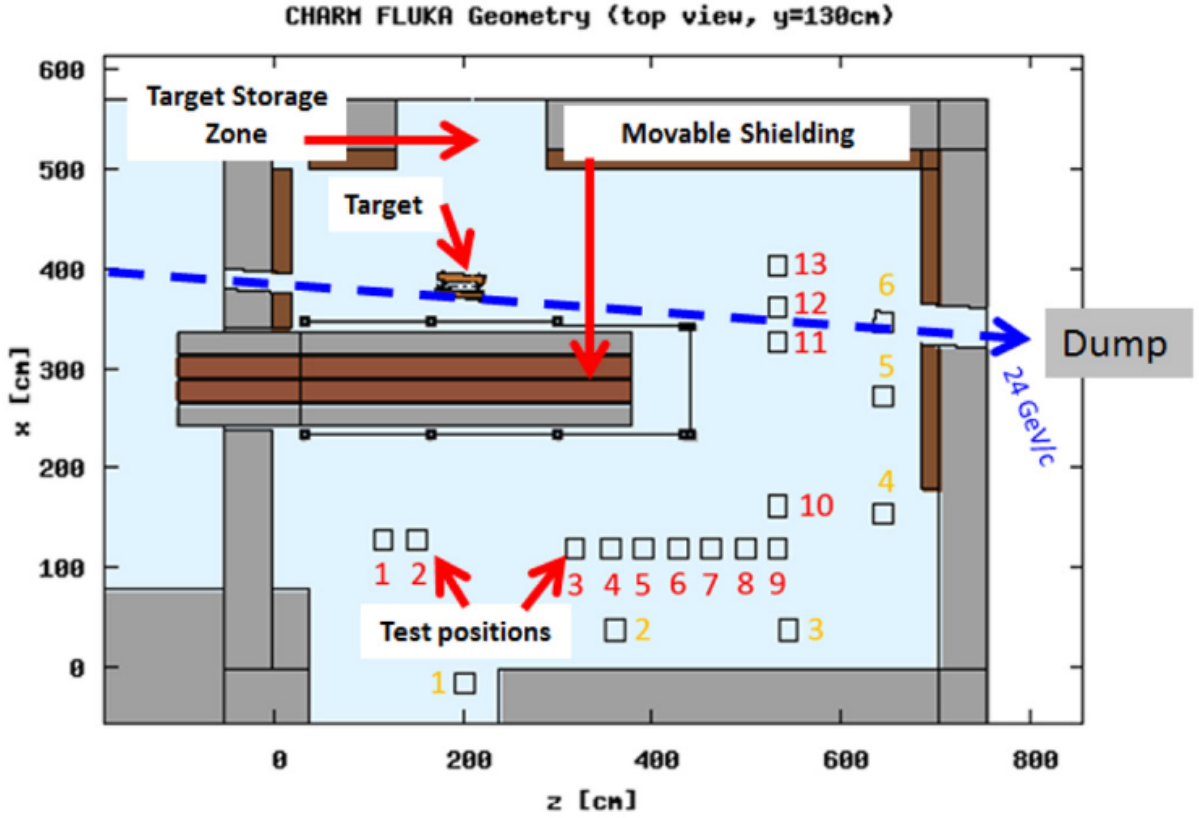


Figure 1: CHARM layout (Image from [6])

3 Explored quantities

3.1 Total Ionising Dose

An important quantity regarding radiation is the Total Ionising Dose (TID). Total Ionising Dose is defined as the energy loss due to ionising radiation per unit mass.

3.2 Fluence Per Unit Lethargy

Another quantity that is explored is fluence per unit lethargy for various particles. Here fluence means the total amount of particles per unit area and lethargy means the logarithm of the ratio of energies of particles before and after collision.

4 Results For Copper Target Configuration

This section covers the results for the CuOOOO configuration. The primary beam energy value of 24 GeV, which corresponds to the energy of the proton beam from the Proton Synchrotron, was hypothetically reduced to: 21, 18, 15, 12, 9 and 1 GeV.

4.1 Total Ionising Dose

This subsection shows the results of the total ionising dose's relation to the primary beam energy. The test locations R1-R13 were explored.

From Figure 2 it can be seen that for the primary beam energy 1 GeV the largest TID value is in the test location R11 and the smallest in R13, which is interesting because both R11 and R13 are right next to R12, which is the location in the beam. For all the other explored beam energy values, however, the highest TID value is in R12, which is quite expected, since R12 is directly in the beam. The locations of the lowest TID values for beam energies 9 GeV - 24 GeV also stay constant and are the ones the furthest from the beam (R1 and R2).

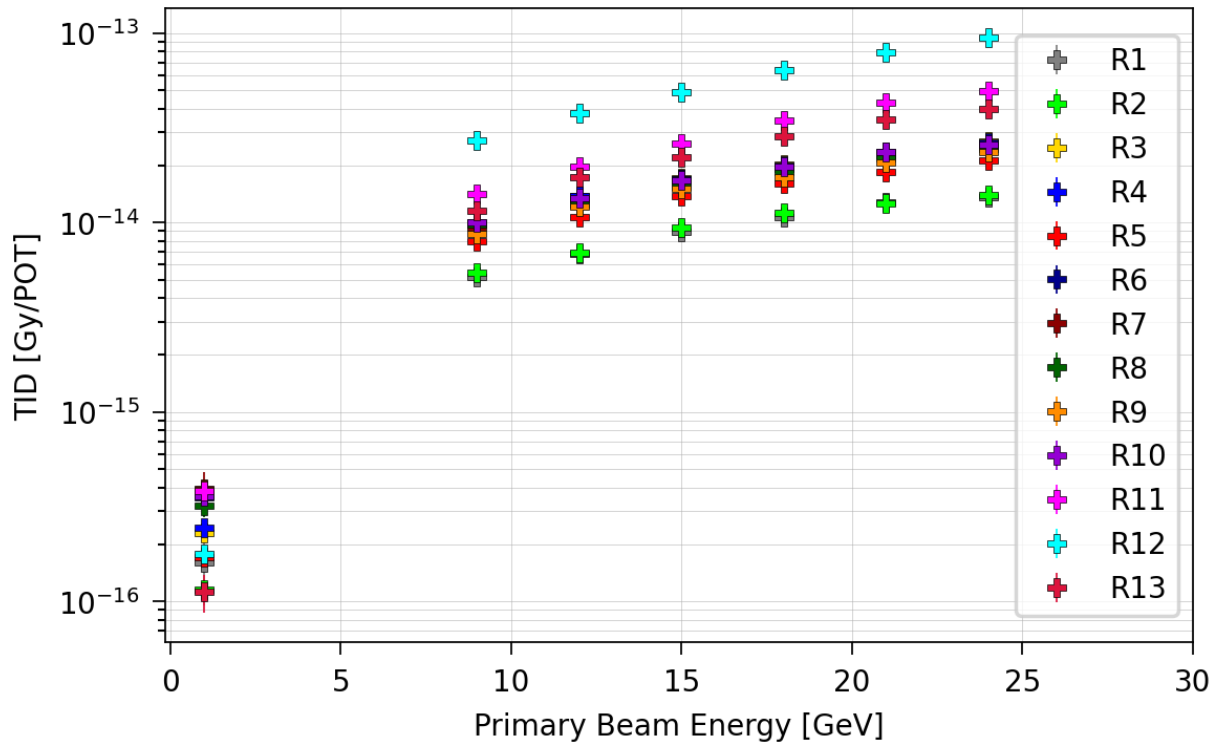


Figure 2: TID's relation to primary beam energy for CHARM R1-R13 test locations.

4.2 Fluence Per Unit Lethargy

This subsection covers the results for the fluence per unit lethargy's relation to the energy of the individual particles' energy. From particles protons, neutrons, photons, electrons, positrons, positive muons and alpha particles were considered. The results are shown for the test locations R12 (subfigure (b) in the following figures), which is in the beam and, R1 (subfigure (a) in the following figures), which is further away from the beam.

4.2.1 Protons' Fluence

Figure 3 shows the fluence for protons. In both locations (R1 and R12) it can be seen that up until about 10^{-1} GeV there is a gradual increase in fluence with the increase in proton's energy but when for R1 it starts decreasing after reaching the maximum, then for R12 the increase just gets slower. That indicates that there are significantly more protons with higher energies in R12, which is an expected result considering R12 is the location in beam. When it comes to the fluence corresponding to the primary beam energy of 1 GeV, it behaves significantly differently from all the other explored primary beam energy values. For R1 it can be seen that the error bars for that configuration are really large regardless of the protons' energy, so it's hard to draw any conclusions from that. For R12, there are some data points with not that large error bars for energies higher than 10^{-1} but as there's only a few of them, it's still hard to draw reasonable conclusions. It can also be noticed that there is no really significant difference in the fluence in regard to the primary beam energy for the beam energies higher than 1 GeV.

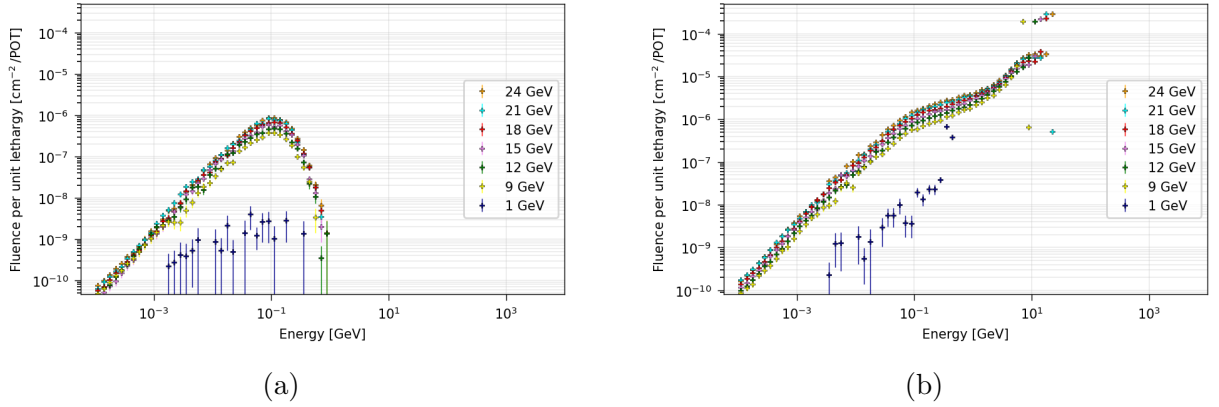
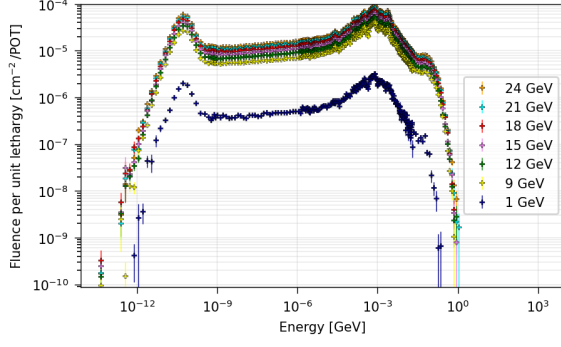


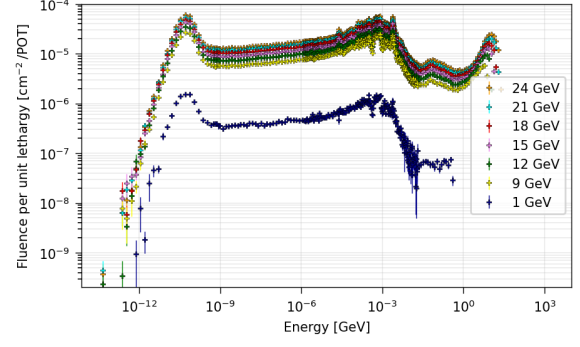
Figure 3: Protons' fluence per unit lethargy's relation to primary energy for different beam energies in test locations a) R1 and b) R12.

4.2.2 Neutrons' Fluence

Figure 4 shows the fluence for neutrons. It can be seen for both locations that there are really few neutrons with energies as low as 10^{-12} GeV and lower and then also for energy values around and over 1 GeV and also the error bars for such particles are quite large. After 10^{-12} GeV up until 10^{-10} GeV with the increase in particle energy the fluence increases then peaking at about 10^{-10} with fluence about $5 \times 10^{-5} \text{ cm}^{-2}/\text{POT}$ after which there is a small decrease in the fluence. From 10^{-10} to 10^{-6} GeV the fluence stays somewhat constant and then increases and peaks again at 10^{-3} GeV, after which it starts quickly decreasing. Though, at about 10^{-3} GeV it increases a bit again, peaking at about $10^{-5} \text{ cm}^{-2}/\text{POT}$, after which for R1 location it quickly decreases but in R12 it increases again peaking at about 10^1 GeV. It can also be seen that the fluence of primary beam energy 1 GeV is significantly lower and with larger error bars than for other primary beam energies.



(a)

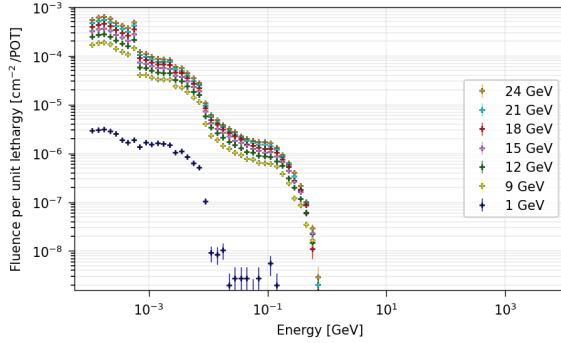


(b)

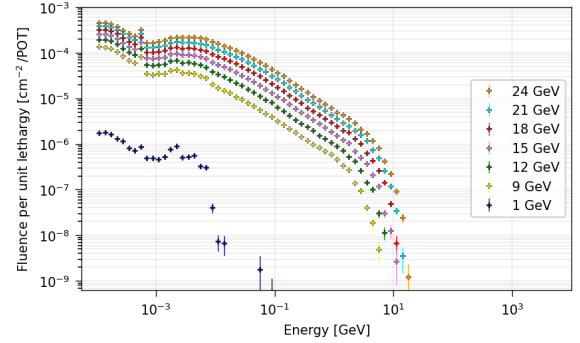
Figure 4: Neutrons' fluence per unit lethargy's relation to primary energy for different beam energies in test locations a) R1 and b) R12.

4.2.3 Photons' Fluence

Figure 5 shows the fluence for photons. It can be seen that most photons are with energies around 10^{-4} - 10^{-3} GeV. With the increase in energy, the fluence decreases significantly. In R1 there are very few particles with energies of about and over 1 GeV, whereas in R12 there are some with energies up to about 10 GeV. In both locations, there is a slight rapid decrease in the fluence at about 8×10^{-3} GeV and in R1 also again at about 10^{-2} GeV. It can also be seen that the change in the primary beam energy has a more significant effect on the fluence in location R12, i.e in the beam. For both locations it can be seen that the fluence for the beam energy 1 GeV is significantly lower than for other primary beam energies and for that energy there are very few photons with energies over 10^{-2} GeV.



(a)



(b)

Figure 5: Photons' fluence per unit lethargy's relation to primary energy for different beam energies in test locations a) R1 and b) R12.

4.2.4 Electrons' Fluence

Figure 6 shows the fluence for electrons. Generally, it can be said that most electrons are with energies between 10^{-4} - 10^{-1} GeV. For configurations with beam energies between 9 - 24 GeV in R1 the fluence at 10^{-4} GeV the fluence is around 10^{-6} cm⁻²/POT after which

with the increase in energy, the fluence increases, peaking at about 10^{-3} GeV, after which it decreases, being significantly smaller with quite large error bars for energies over about 10^{-1} GeV. Also there are really few electrons for the primary beam energy of 1 GeV configuration. For R12, the fluence at 10^{-4} GeV is slightly larger than for R1. After that point it slowly and very slightly increases with the increase in electrons' energy but such a peak as for R1 is not prominent. After about 10^{-2} GeV, the fluence starts decreasing with an increasing pace until at about 10 GeV the fluence has decreased to $10^{-8} - 10^{-9} \text{ cm}^{-2}/\text{POT}$ and for such electrons the error bars are already really big.

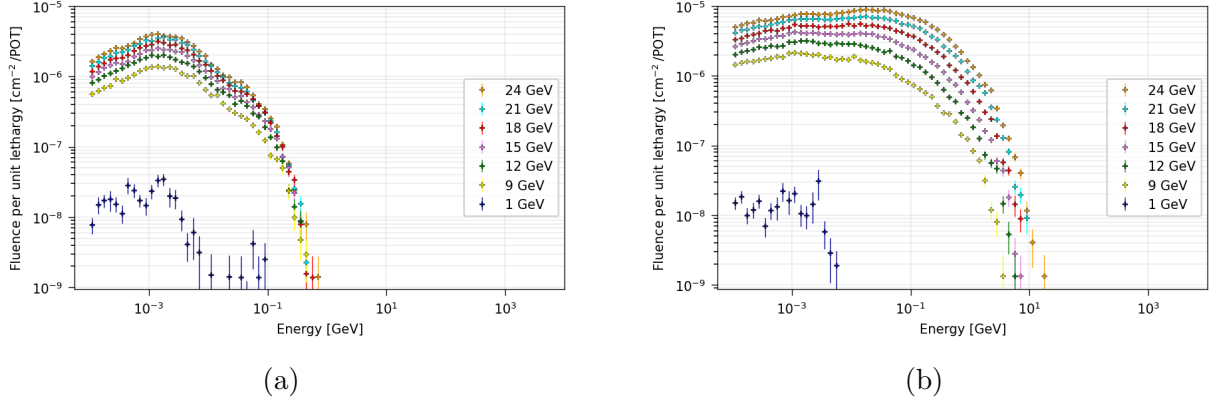


Figure 6: Electrons' fluence per unit lethargy's relation to primary energy for different beam energies in test locations a) R1 and b) R12.

4.2.5 Positrons' Fluence

Figure 7 shows the fluence for positrons. The general shape of the graphs is similar, gradually increasing, reaching a maximum and then decreasing again. For energies up to 10^{-3} GeV the behaviour in locations R1 and R12 is really similar, indicating an increase in fluence with the increase in positrons' energy. In R1 the fluence peaks at about 10^{-2} GeV, whereas in R12 the fluence reaches its maximum at slightly higher energies close to 10^{-1} GeV. After the maximum, the fluence decreases for both locations. It can be seen that there are really few positrons of energies larger than 1 GeV in R1 and 10 GeV in R12. Interestingly, there is again a noticeable difference in the effect of primary beam energy on the fluence. The effect in R1 and R12 is really similar for positrons of smaller energies but when it comes to energies larger than 10^{-2} GeV then the effect is significantly larger in R12 compared to R1. Again, it's clearly noticeable that the behaviour for the primary beam energy of 1 GeV is completely different than for all the other energies and the error bars of the positrons of that configuration are really large, making it hard to draw any conclusions about them.

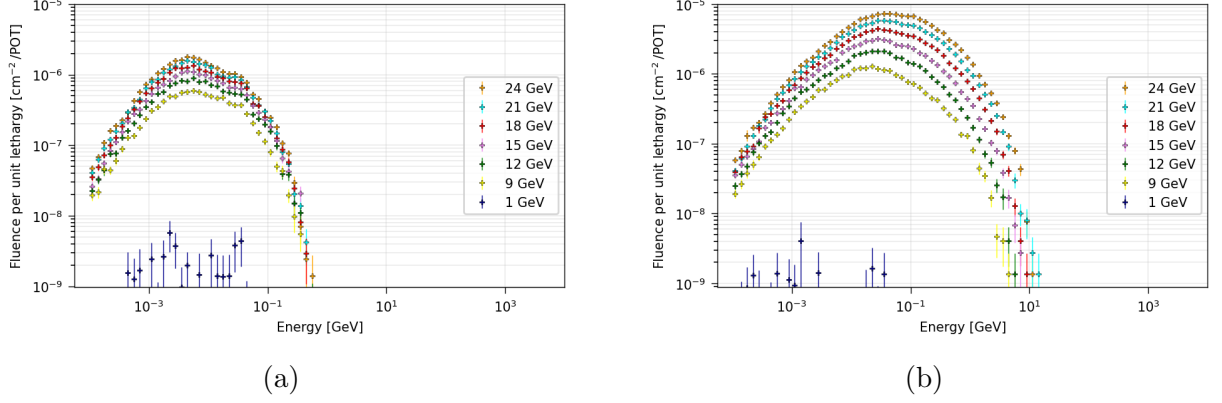


Figure 7: Positrons' fluence per unit lethargy's relation to primary energy for different beam energies in test locations a) R1 and b) R12.

4.2.6 Positive Muons' Fluence

Figure 8 shows the fluence of muons. It can be seen that for muons the fluence peaks at about 10^{-7} GeV which is smaller than for all the previously mentioned particles. For smaller energies, the behaviour in R1 and R12 is really similar. The error bars for the muons with energies lower than 10^{-2} GeV are really large, so not much can be concluded about them. From that energy in both locations, the fluence increases, peaking at 10^{-1} GeV for R1 and at 10^{-2} GeV for R12. After the peak, there is a quite quick decrease for both locations and it can be seen that the error bars for particles after the peak are quite large and increasing in size with the further increase in energies. When it comes to the effect of the change in primary beam energy on the fluence, it can be noticed that close to the energies corresponding to the peak, there is a more significant difference in the effect for R12 in comparison to R1. For muons the fluence that correspond to the primary beam energy of 1 GeV seems to be basically nonexistent.

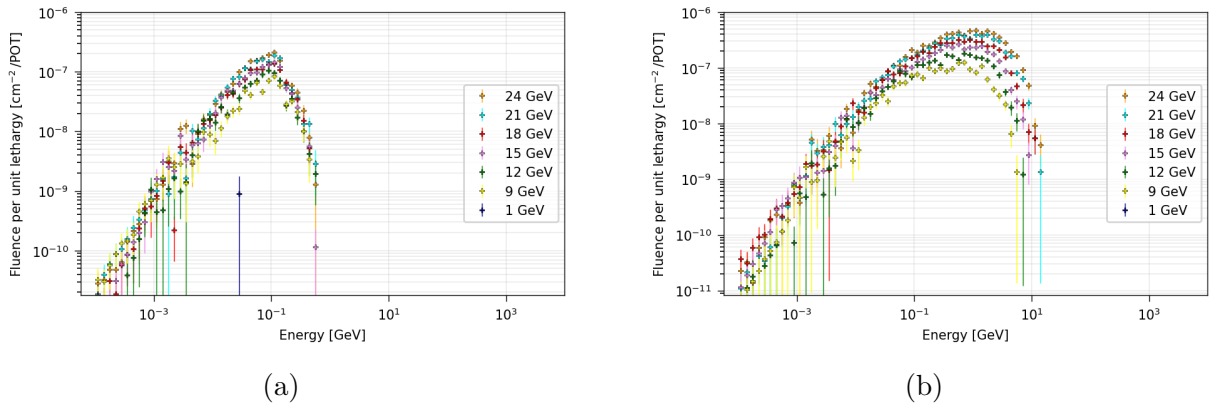


Figure 8: Muons' (positive) fluence per unit lethargy's relation to primary energy for different beam energies in test locations a) R1 and b) R12.

4.2.7 Alpha Particles' Fluence

Figure 9 shows the fluence of alpha particles. It can be seen that the error bars are really large for both locations and for whichever energy values. However, it is worth mentioning that in R12 for energies between 10^{-3} and 10^{-1} GeV, the error bars aren't that large but still too large to draw any reasonable conclusions.

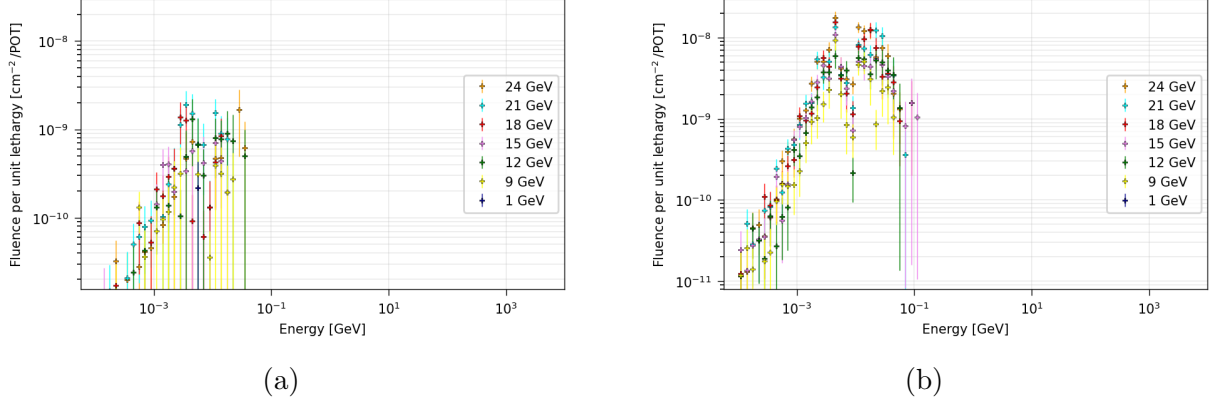


Figure 9: Alpha particles' fluence per unit lethargy's relation to primary energy for different beam energies in test locations a) R1 and b) R12.

5 Results For No Target Configuration

This section covers the results for the NTOOOO configuration. For the primary beam energies, the same values were explored as for the copper target configuration.

5.1 Total Ionising Dose

This subsection shows the results of the total ionising dose's relation to the primary beam energy. Total Ionising Dose is defined as the energy loss due to ionising radiation per unit mass. From test locations again positions R1-R13 were considered.

From Figure 10 it can be seen that the total ionising dose doesn't change much with the change in the primary beam energy in R12 and the neighbouring locations R11 and R12. When it comes to the other locations further away from the beam, then there are slightly more fluctuations in regard to the primary beam energy. For most beam energies the location with the smallest TID is either R1 or R2, which is reasonable, considering they are the furthest away from the beam. Interestingly, for 12 GeV the smallest TID is in R3, followed by R5. The highest TID values for all beam energies are in R12, followed by R11 and R12. There is a big difference in the TID values for R12, which are about $5 \cdot 10^{-13}$, R11 and R13, which are between 10^{-15} and $5 \cdot 10^{-15}$ and other locations which are mostly between 10^{-17} and 10^{-16} Gy/POT.

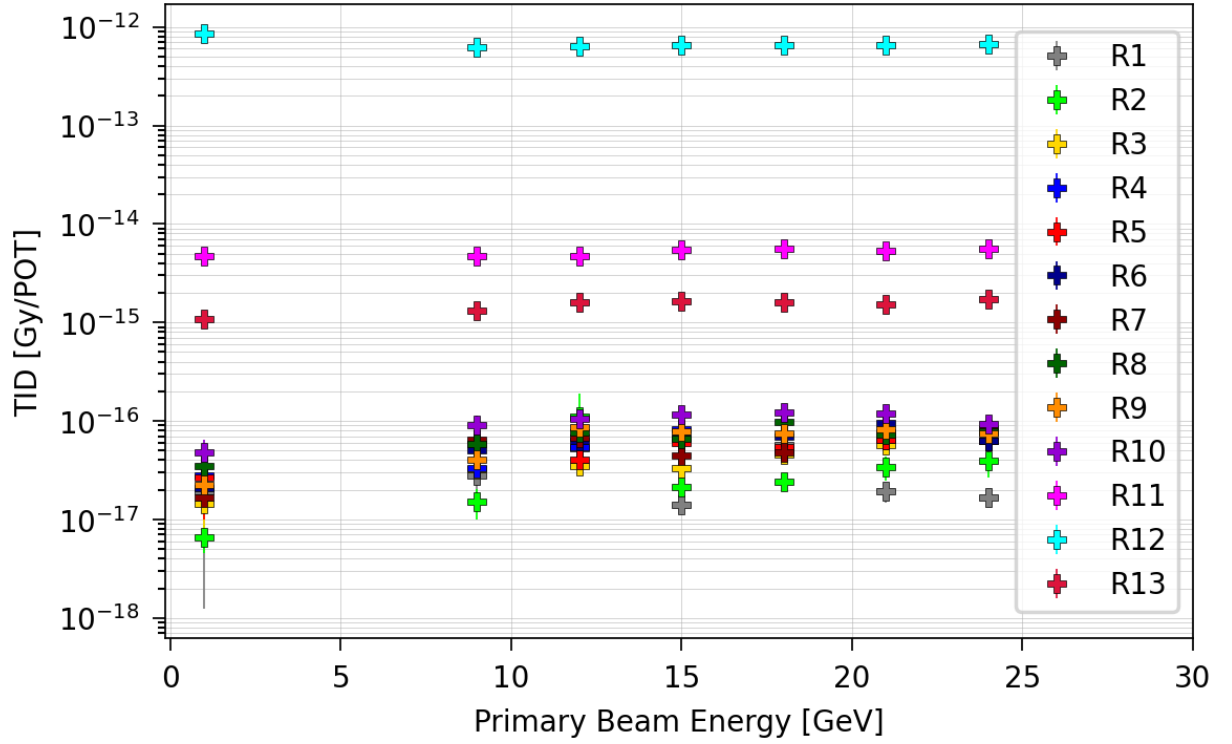


Figure 10: TID's relation to primary beam energy for CHARM R1-R13 test locations.

5.2 Fluence Per Unit Lethargy

This subsection covers the results for the fluence per unit lethargy's relation to the energy of the individual particles' energy. The exact same particles were explored as for the copper configuration. The results are shown for the test locations R12 (subfigure (c) in the following figures), which is in the beam, R11 and R13 which are right next to the beam (subfigures (b) and (d) accordingly) and R10 which is further away from the beam.

5.2.1 Protons' fluence

Figure 11 shows the fluence for protons. Generally, it can be seen that most protons have energies between 0.1 and 10 GeV. The difference in fluence in different locations is remarkable, most interestingly there is a large difference in the shape of the graph between R11 and R13, with there being significantly more higher energy protons present in R11. In R11 and R12 the difference in fluence in regard to the primary beam energy is not significant, however, in R13 it is slightly more significant. For the test location R10, it is difficult to draw any conclusions, because the error bars are relatively large. It can be said, however, that most of the protons have energies around 0.1 GeV. For the test locations R11-R13, there is a steady increase in proton fluence the larger the primary energy is, with the most energetic protons having energies close to 10 GeV. When for R11, there is no decrease, then for the test location R12 at energies around 10 GeV, the proton fluence starts to fall again. For the test location R13, starting at primary energies of 0.1 GeV, the fluence plateaus and

stays constant until 10 GeV, after which the fluence starts to fall again. Also, interestingly, in locations R11- R13 there are a few data points at about 0.5 GeV for primary beam energy 1 GeV, which are remarkably higher than the ones for all the other primary beam energies.

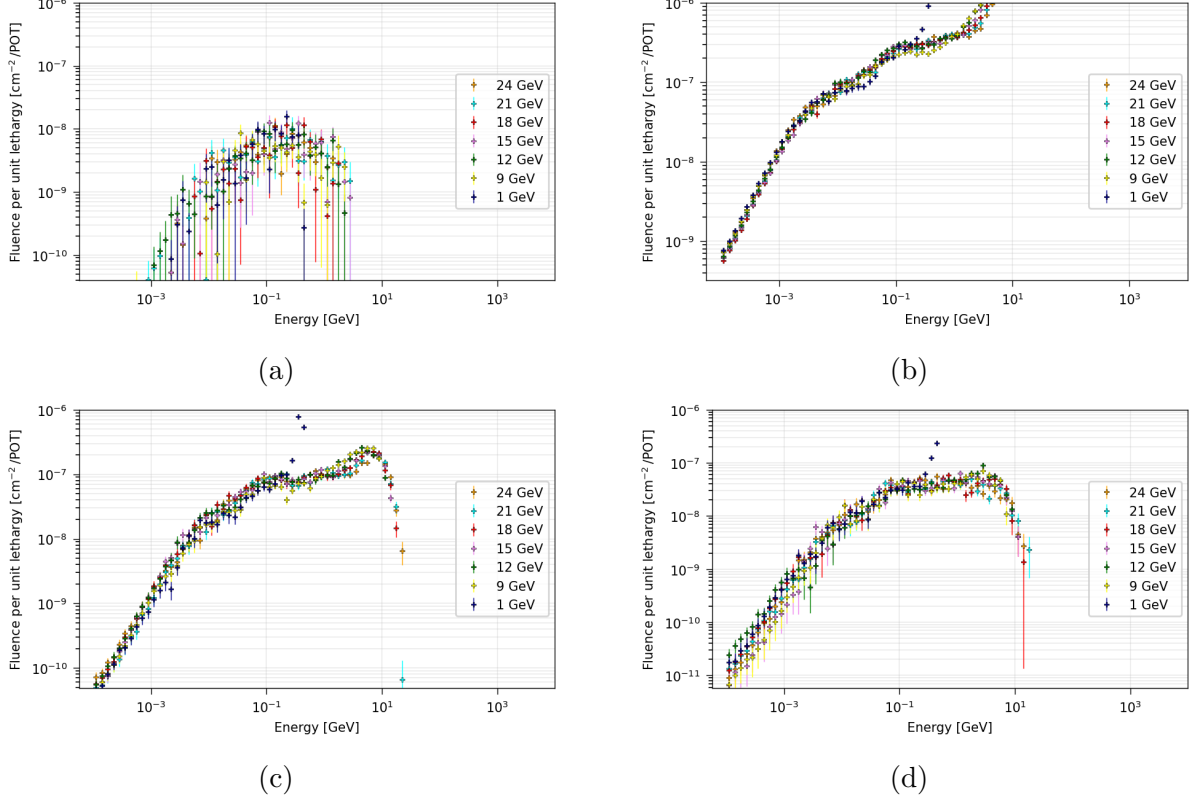


Figure 11: Protons' fluence per unit lethargy's relation to primary energy for different beam energies in test locations a) R10, b) R11, c) R12 and d) R13.

5.2.2 Neutrons' Fluence

Figure 12 shows the fluence for neutrons. It can be seen that for test locations R11-R13 the general behaviour for all primary beam energies, except for again 1 GeV (for which the error bars are really large, making hard to draw any conclusions whatsoever), is fairly similar, with the main difference being in the height of the peaks. There are very few neutrons present with energies about 10^{-12} GeV and lower and the error bars for those fluences are quite large. With the increase in energy, the fluence increases, reaching its peak at about 10^{-10} GeV at about $10^{-6} \text{ cm}^{-2}/\text{POT}$, after which there is a small decrease until about 10^{-9} GeV, followed by a slow increase until 10^{-5} GeV. There are two sharp peaks at about $5 \cdot 10^{-5}$ GeV and 10^{-4} GeV with a significant decrease between them. In R12 the peaks are at about $10^{-4} \text{ cm}^{-2}/\text{POT}$, in R11 slightly lower and in R13 at about $10^{-5} \text{ cm}^{-2}/\text{POT}$. After the peak at 10^{-4} GeV, the fluence decreases again, having a small peak at about 0.1 GeV and another one at about 10 GeV. There are very few neutrons with energies larger than about 10 GeV. For R10, the behavior is really similar until 10^{-9} GeV. After that there is a really slow

increase until 10^{-3} GeV, followed by a quick decrease and another smaller peak at about 0.1 GeV.

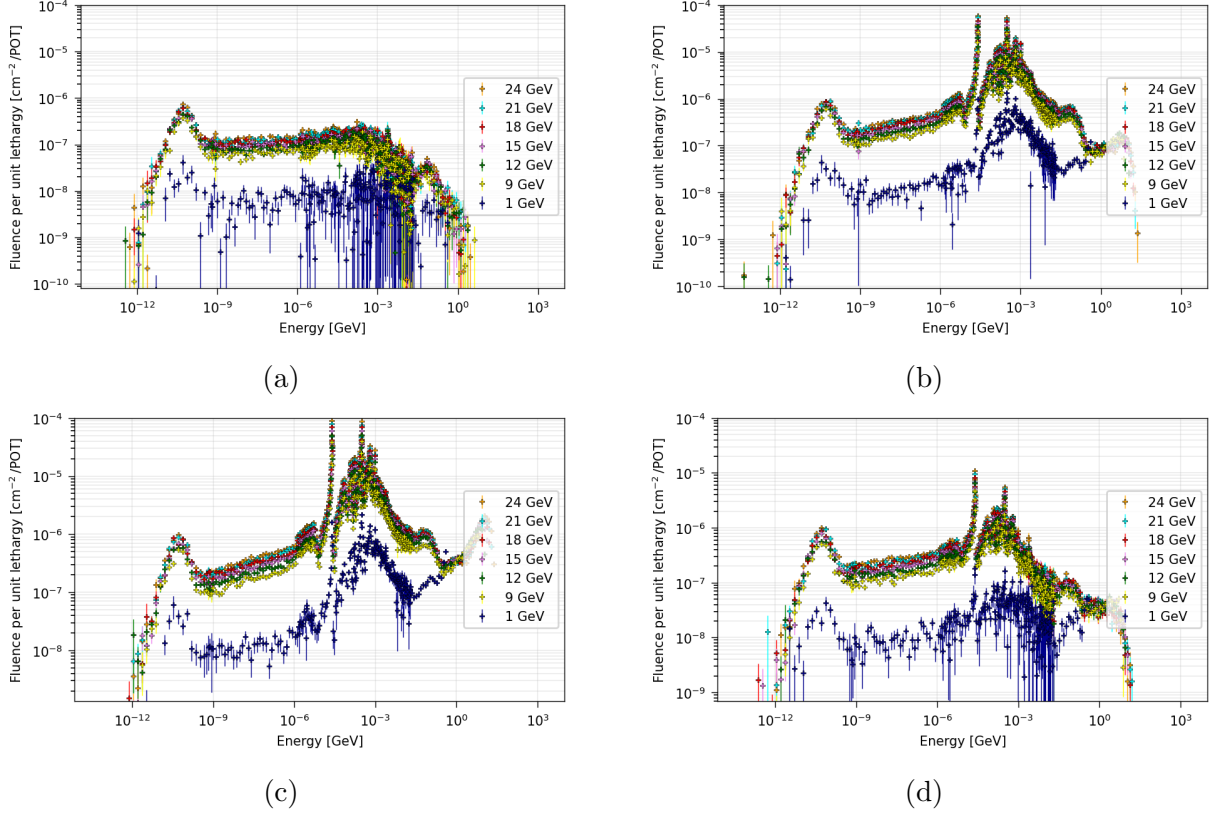


Figure 12: Neutrons' fluence per unit lethargy's relation to primary energy for different beam energies in test locations a) R10, b) R11, c) R12 and d) R13.

5.2.3 Photons' Fluence

Figure 13 shows the fluence for photons. It can be seen that the general behaviour of there being 2 noticeable peaks for the fluence is visible in all locations, although the peaks are present at quite different fluence values and in R10, the peak at about 10^{-2} GeV is barely noticeable. In all test locations, except for R12, most of the photons have energies between 10^{-4} and 10^{-2} GeV. In R12, however, there are a lot of higher energy (from 0.1 GeV up until almost 10 GeV) present as well. Expectedly, the highest photon fluence (slightly over 10^{-6} cm⁻²/POT) with the smallest error bars is the one in R12, however quite interestingly the smallest is not in R10, which is the furthest from the beam, but instead in R11. When it comes to the 1 GeV primary proton beam energy, then as previously, the corresponding fluence behaves quite differently from the higher beam energies and has really large error bars, throughout the photon energy range.

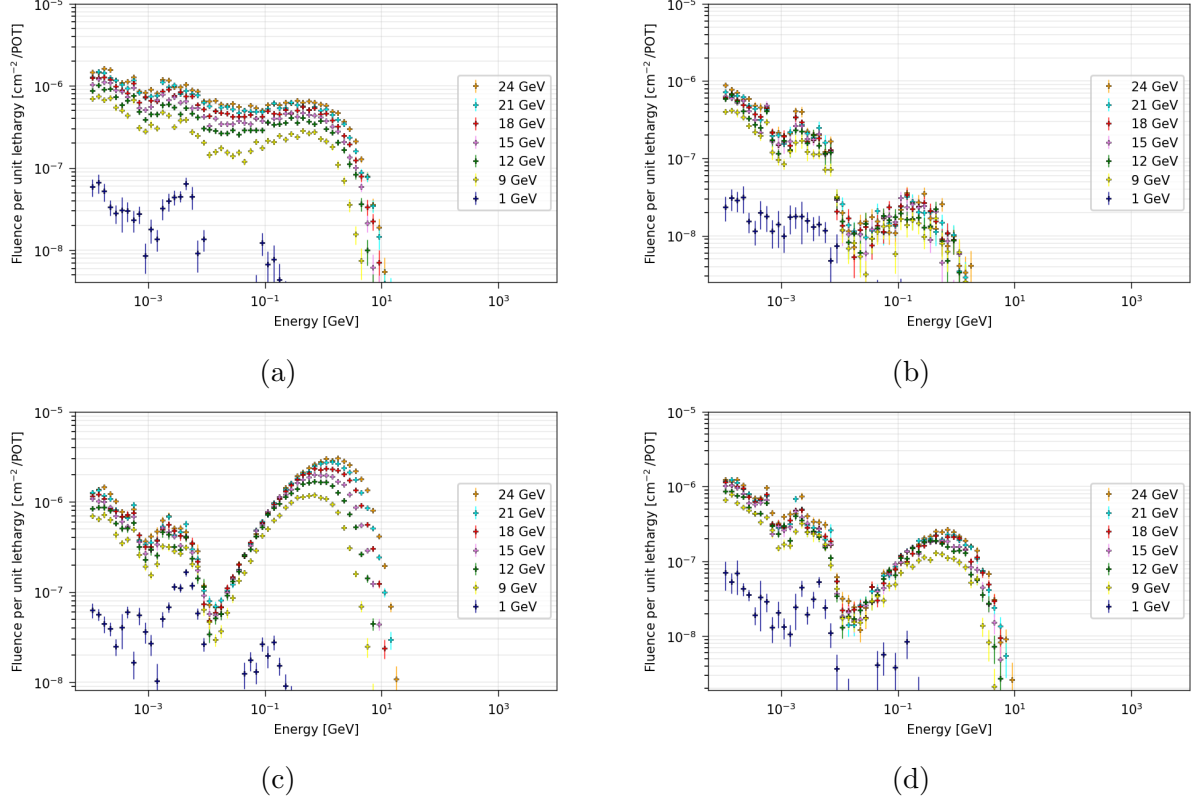


Figure 13: Photons' fluence per unit lethargy's relation to primary energy for different beam energies in test locations a) R10, b) R11, c) R12 and d) R13.

5.2.4 Electrons' Fluence

Figure 14 shows the fluence for electrons. It can be seen that most electrons have energies 10^{-4} and 10^{-2} GeV and there are really few electrons with energies over 0.1 GeV and their error bars are quite significant. Expectedly, the highest fluence of about $10^{-5} \text{ cm}^{-2}/\text{POT}$ is present in the test location R12, with the neighbouring locations R11 and R13 having about 1 order of magnitude lower maximum fluence values. For R12 there is a steady decrease in fluence with the increase in electron's energies, however, for R11 and R13 there is a small peak at about 5×10^{-4} GeV. For R12 and R13 there is almost no difference in the fluence in regard to the primary beam energies until energies lower than 0.1 GeV, for R10 and R11 it can only be said for energies lower than 0.01 GeV. After these values, the differences are noticeable but also the error bars are too large to draw conclusions for all locations except for R11, where the error bars are still larger than for lower energies but not as large as in other locations. An interesting phenomenon is noticeable in R11-R13 for electron energies 10^{-4} - 10^{-3} GeV, where the fluence for the primary beam energy 1 GeV is clearly larger than for the other primary beam energies.

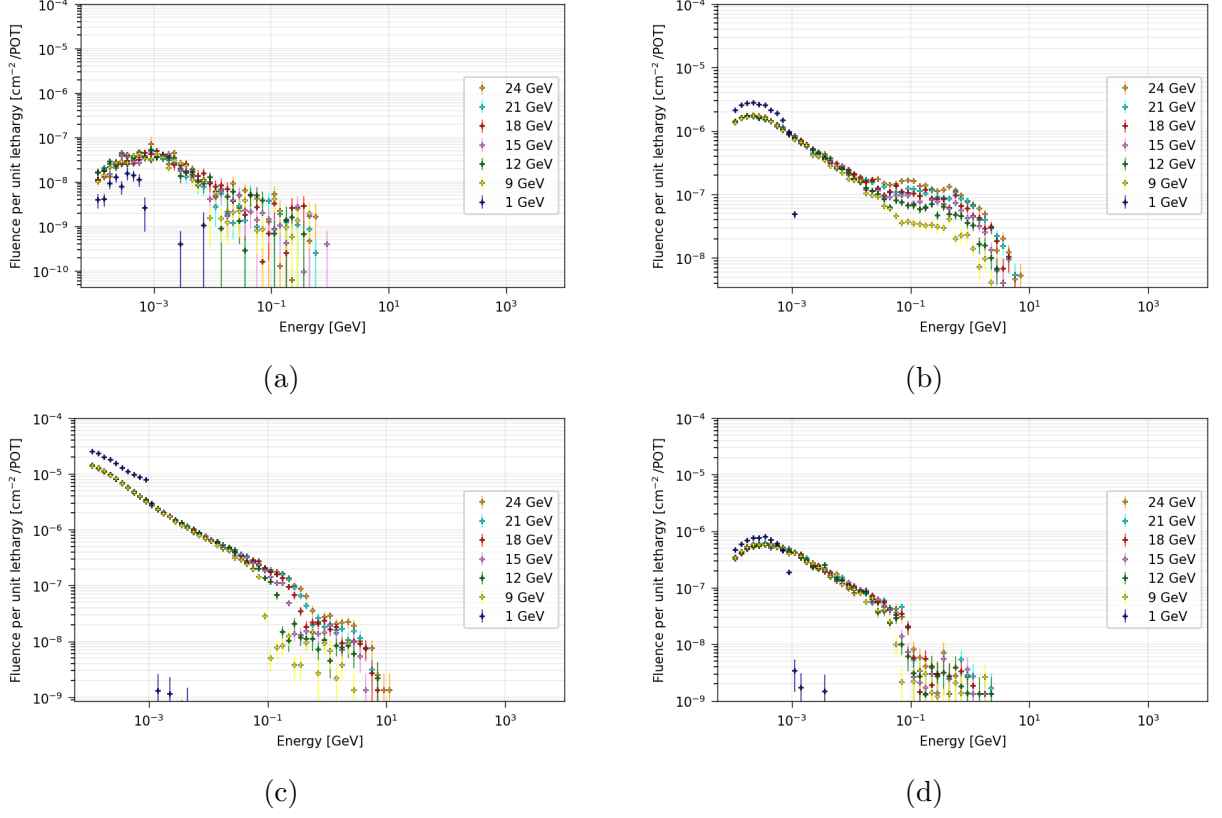
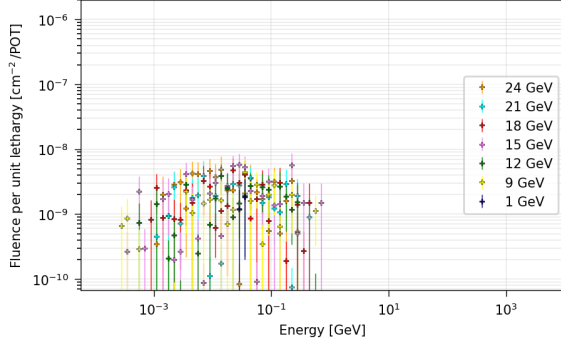


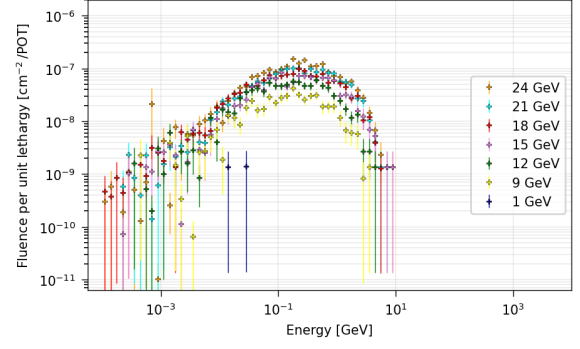
Figure 14: Electrons' fluence per unit lethargy's relation to primary energy for different beam energies in test locations a) R10, b) R11, c) R12 and d) R13.

5.2.5 Positrons' Fluence

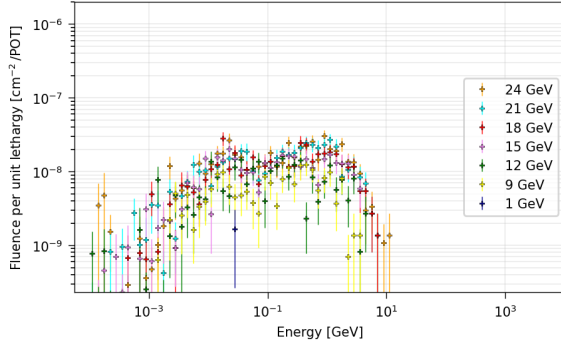
Figure 15 shows the fluence for positrons. It can be seen that for all locations other than R11 the error bars are extremely large for whichever positron' energies and whichever primary proton beam energies, so it is not really possible to draw any conclusions about them. In R11 the error bars are really large for energies lower than about 10^{-2} GeV and then again for energies close to 10 GeV. Between these energies there is a clear peak in the fluence at about 0.5 GeV at about $10^{-7} \text{ cm}^{-2}/\text{POT}$. It can be concluded that in R11 most positrons have energies between about 0.01 and 5 GeV. Also, there seems to be significant difference in the fluence values in regard to the primary beam energy. For the primary beam energy 1 GeV there are too few data points to draw any conclusions about the positrons' fluence.



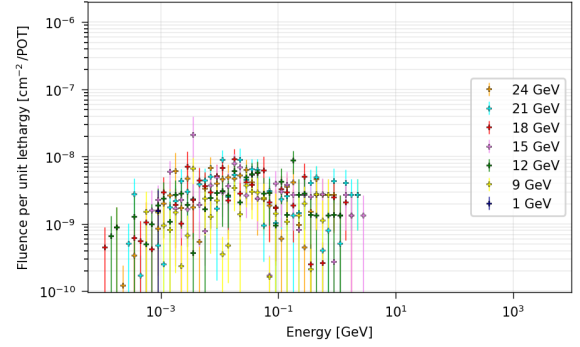
(a)



(b)



(c)



(d)

Figure 15: Positrons' fluence per unit lethargy's relation to primary energy for different beam energies in test locations a) R10, b) R11, c) R12 and d) R13.

5.2.6 Positive Muons' Fluence

Figure 16 shows the fluence of muons. It can be seen that for whichever locations and energies, the error bars for the fluence are extremely large, making it hard to draw any conclusion about muons' fluence whatsoever.

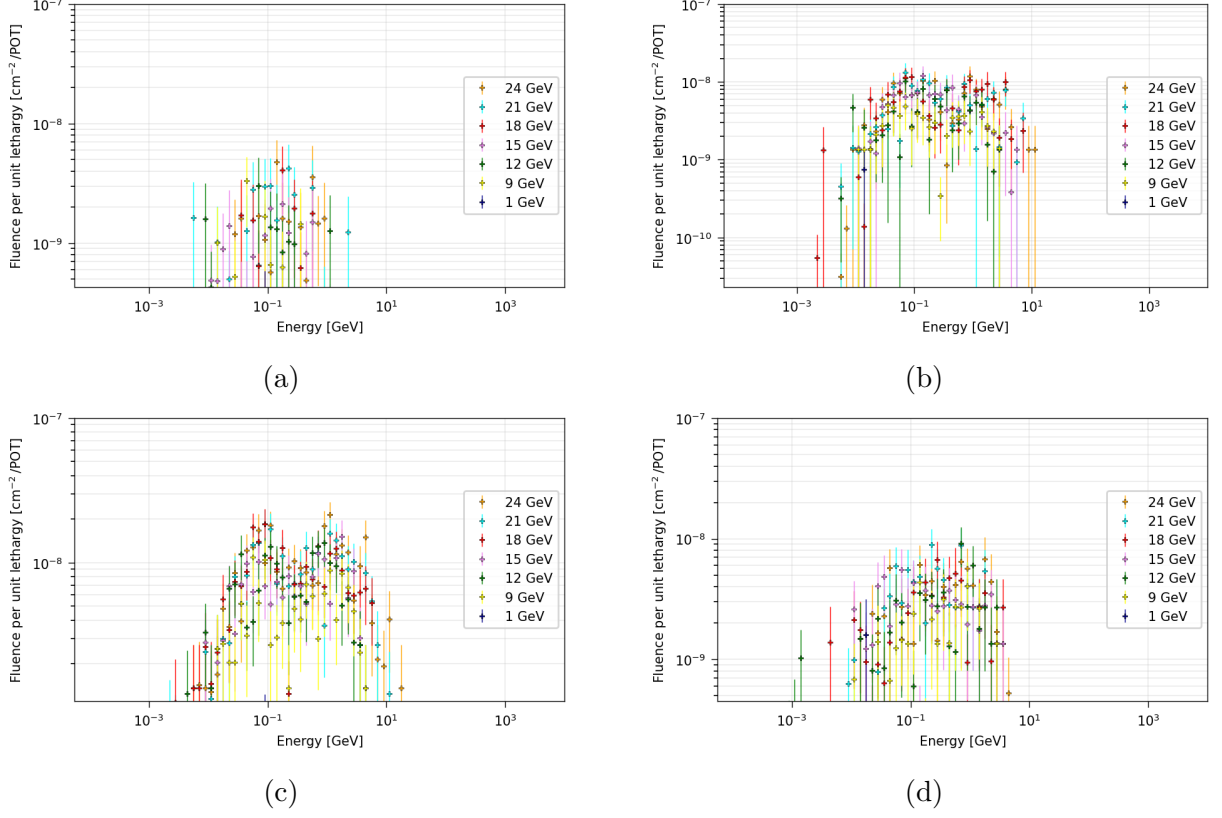


Figure 16: Muons' (positive) fluence per unit lethargy's relation to primary energy for different beam energies in test locations a) R10, b) R11, c) R12 and d) R13.

5.2.7 Alpha Particles' Fluence

Figure 17 shows the alpha particles' fluence. It can be seen that for R10 there are no data points at all and for R11 and R13 the error bars are again too large to draw reasonable conclusions. For R12 the error bars are also quite large but not as large for the other locations. It can be seen that in R12 the fluence at 10^{-4} GeV is about $10^{-10} \text{ cm}^{-2}/\text{POT}$ which increases peaking at about 10^{-2} GeV at about $10^{-10} \text{ cm}^{-2}/\text{POT}$ after which there is a sudden decrease, followed by a sudden increase. At alpha particles' energies around 0.1 GeV the fluence has lowered and the error bars are already too big to draw any conclusions.

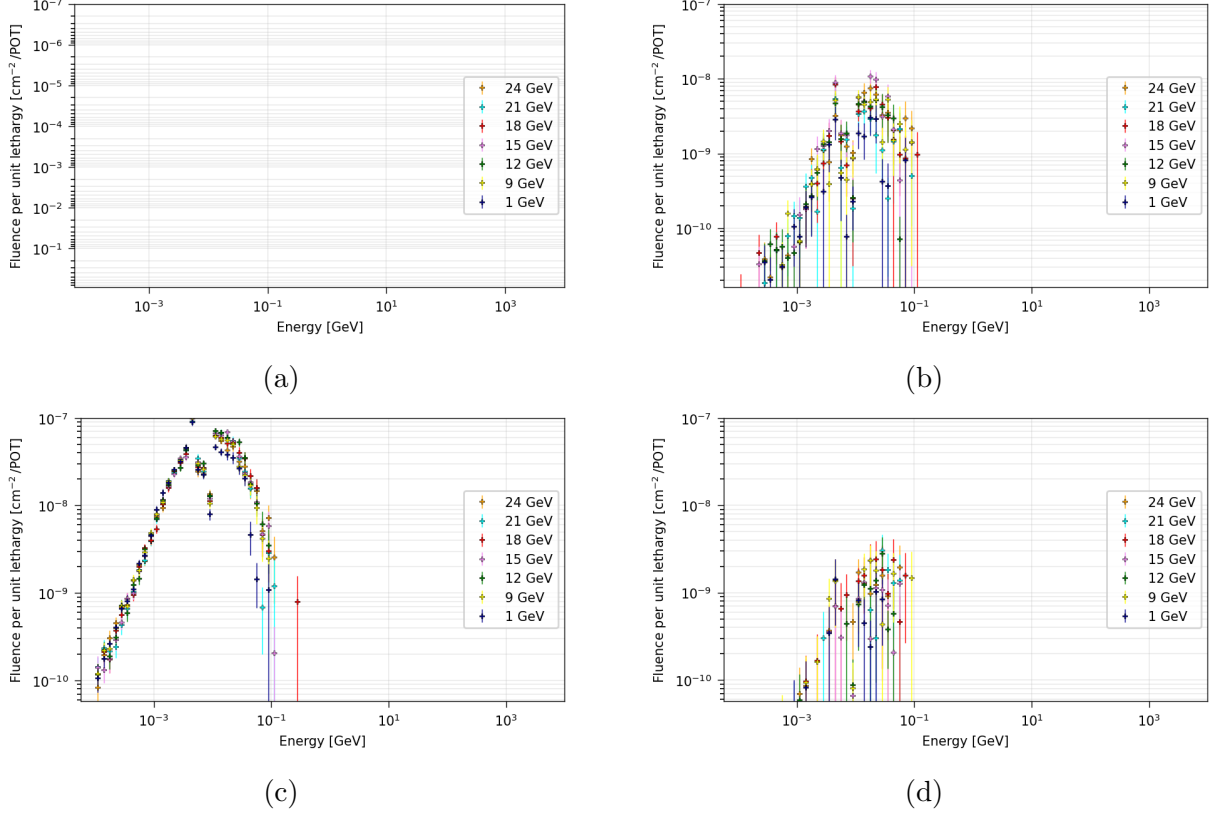


Figure 17: Alpha particles' fluence per unit lethargy's relation to primary energy for different beam energies in test locations a) R10, b) R11, c) R12 and d) R13.

6 Conclusion

The TID's and the fluence per unit lethargy's relation to different particle energies were simulated using FLUKA software and then analysed for different particles, primary beam energies, test locations and for both copper target and no target configurations. When for the target configuration there was a noticeable increase in the TID with the increase in the primary beam energy then for the no target configuration the TID stayed almost constant with the increase in the primary beam energy in all the more important locations closer to the beam. For the target configuration for all the explored particles it could be seen that in the test location in the beam (R12) there was a more significant difference in the fluence per unit lethargy in regard to the particle energy compared to the test location R1 (further away from the beam). For the no target configuration an interesting phenomenon was present where the behaviour of the fluence per unit lethargy was different in the test locations R11 and R13, which are both close to the beam, but on different sides of it.

References

- [1] J. Mekki et al. CHARM: A Mixed Field Facility at CERN for Radiation Tests in Ground, Atmospheric, Space and Accelerator Representative Environments. *IEEE Trans. Nucl. Sci.*, 63(4):2106–2114, 2016. doi: 10.1109/TNS.2016.2528289.
- [2] D. Prelipcean et al. Benchmark between measured and simulated radiation level data at the mixed-field charm facility at cern. *IEEE Transactions on Nuclear Science*, 69(7): 1557–1564, 2022. doi: 10.1109/TNS.2022.3169756.
- [3] FLUKA website. URL <https://fluka.cern>.
- [4] FLUKA.CERN Collaboration. *New Capabilities of the FLUKA Multi-Purpose Code*. 2022. URL <https://www.frontiersin.org/articles/10.3389/fphy.2021.788253/full>.
- [5] G. Battistoni et al. Overview of the fluka code. *Annals of Nuclear Energy*, 82:10 – 18, 2015. ISSN 0306-4549. doi: <https://doi.org/10.1016/j.anucene.2014.11.007>. URL <http://www.sciencedirect.com/science/article/pii/S0306454914005878>.
- [6] A. Thornton. CHARM Facility Test Area Radiation Field Description, Apr 2016. URL <https://cds.cern.ch/record/2149417>.
- [7] A. Infantino. FLUKA Monte Carlo Modelling of the CHARM Facility’s Test Area: Update of the Radiation Field Assessment, September 2017. URL <https://cds.cern.ch/record/2291683>.